Femtosecond electron-lattice thermalization dynamics in a gold film probed by pulsed surface plasmon resonance

Alexandre A. Kolomenskii,* Ryan Mueller, Joshua Wood, James Strohaber, and Hans A. Schuessler

Department of Physics & Astronomy, Texas A&M University, College Station, Texas 77843-4242, USA

*Corresponding author: a-kolomenski@physics.tamu.edu

Received 28 June 2013; revised 25 September 2013; accepted 27 September 2013; posted 1 October 2013 (Doc. ID 193090); published 17 October 2013

The dynamics of electronic excitations and their relaxation in a gold film is studied on the femtosecond time scale with a pump–probe technique. For the pump beam we use pulses with wavelengths centered at 800 nm, 400 nm or both. The surface plasmon resonance (SPR) in Kretschmann's configuration is used as a sensitive and fast-response probe of the dynamics of the dielectric properties of the gold film. The quantity that is monitored is the intensity of the reflected light at an incidence angle close to the SPR. With changes of the dielectric properties induced by the pump beam and during subsequent relaxation, the amount of the reflected light of the probe beam, sent with a variable delay, also changes, thus providing information on the temporal characteristics of the thermalization process. Special features of SPR probing with short pulses are also accounted for in this work. The thermalization of the electronic subsystem and energy transfer to the lattice are discussed in connection with the two-temperature relaxation model that takes into account temperature dependences of the electronic heat capacity and the electron–phonon coupling.

OCIS codes: (300.6530) Spectroscopy, ultrafast; (310.6860) Thin films, optical properties; (240.6680) Surface plasmons.

http://dx.doi.org/10.1364/AO.52.007352

1. Introduction

Ultrafast laser pulses can efficiently excite the electronic subsystem of a metal and allow monitoring of the fast thermalization dynamics after the excitation. The possibility to create transient excited states in materials is also important for developing ultrafast opto-electronic devices, such as light switches controlling light by light. There is a time hierarchy of different dynamic processes during an ultrafast excitation of a metal [1–4]: (1) The pump laser pulse excites electrons and creates a non-Fermi distribution in the conduction band. (2) The nonequilibrium electronic subsystem moves toward a quasi-equilibrium distribution with an effective temperature of the electrons that can be much higher than the temperature of the lattice. The redistribution of the energy of the excited electrons takes place via electron–electron scattering within about 100–300 fs. (3) The transfer of energy from the electrons to the lattice takes place on a picosecond time scale due to the electron–phonon interaction. The latter process is often described by the two-temperature model (TTM). Detailed calculations based on a Boltzmann collision integral [2,4,5] and direct measurements of the electron thermalization by time-resolved photoemission spectroscopy [6] and two-pulse-correlation femtosecond thermionic emission [7] reveal the limitations for the applicability of TTM and elucidate the role of electron–electron and electron–phonon interactions in the thermalization process. (4) Finally, at longer

1559-128X/13/307352-08$15.00/0

times the thermalization of the lattice with the environment takes place, and after this process is completed, the system comes to a true equilibrium.

The dynamics of the dielectric properties were previously studied by using a combination of reflection and transmission [2,8]. It was also demonstrated that surface plasmons (SPs) can serve as a sensitive probe of metal dielectric properties [9,10]. The SP propagation constant depends on the dielectric properties of the materials in the vicinity of the metal boundary within the penetration depth of the electromagnetic field. Since the electronic response is fast, SPs allow probing the changes of the dielectric properties and fast dynamics on a very short time scale; the response time depends on the light wavelength and varies from a few femtoseconds to 100 fs [11–13]. In particular, a pump–probe experiment with a probe coupled to SPs via a grating [12] shows the potential of this scheme for ultrafast optical switching.

In this work we use SPs to monitor the dynamics of the electronic excitations and their relaxation in gold films on the femtosecond time scale with a pump–SP probe technique. We show that the detection with SPs is about 200-fold more sensitive than a standard probing with surface reflection. Correspondingly, large changes in the reflected intensity, observed at the SPR, are a promising approach to realization of fast optical switching. For measuring the relaxation dynamics, the intensity of the reflected light at an incidence angle close to the SPR angle is monitored. The amount and angular distribution of the reflected light of the probe beam, as a function of delay, depend on the changes of the dielectric properties induced by the pump beam and the relaxation process. Measuring the probe response at different delays provides information on the temporal characteristics of the thermalization. SP excitation with short pulses has peculiarities related to employment of broadband radiation that are also accounted for in this work. In addition, we show that by an appropriate selection of the angular detection interval, one can predominantly measure the changes in the real or imaginary parts of the metal dielectric constant. The thermalization of the electronic subsystem and the energy transfer to the lattice are discussed in connection with the two-temperature relaxation model taking into account temperature dependences of the electronic heat capacity and the electron–phonon coupling parameter.

2. Experimental Apparatus and Procedures

A. Experimental Setup

Amplified laser pulses with a duration of 50 fs and energy of 1 mJ at 1 kHz (Spitfire, Spectra Physics) were split into two sub-beams (see Fig. 1): the main part was used as a pump to produce electronic excitations in a gold film directly at 800 nm or by doubling the frequency with a beta-barium borate crystal and using the second harmonic at 400 nm. For a selection of the desired wavelength a 3 mm red or blue (RG715 or BG38, Schott Inc.) filter was inserted in the beam path before the gold film. When using both wavelengths the filter was removed, and the delay between 800 and 400 nm pulses was determined by their different delays when passing the focusing system of lenses L2 and L3. The smaller portion of the 800 nm beam with about 1 μJ pulse energy was used as the SP probe in the Kretschmann configuration with a prism [14]. Figure 1 shows also the arrangement with a prism used for the SPR observation. Each second pump pulse was blocked by a chopper to enable noise background subtraction and efficient extraction of the signal at 500 Hz. The probe

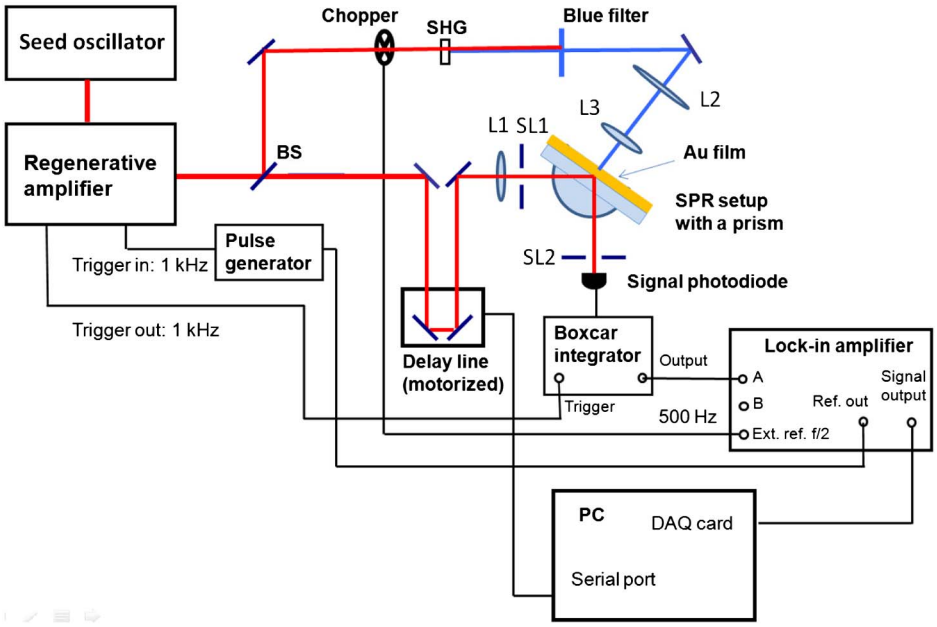

Fig. 1. Schematic of the experimental setup.

pulses were measured by a photodiode, and this signal was integrated by a boxcar and sent to a lock-in amplifier, set to external referencing by the chopper at $f/2$. The reference from the lock-in at 1 kHz was sent to a pulse generator to produce a trigger for the laser.

The probe beam passed through a motorized computer-controlled delay line and was focused with a cylindrical lens and directed through a slit SL1 and a hemicylindrical prism on the area of the gold film subjected from the other side to the action of the pump pulse. The size of the probe beam spot was chosen to be 0.2 mm and smaller than the size of the pump beam, set to about 0.4 mm. Focusing with a cylindrical lens provided a range of incidence angles centered on the SPR angle of 42.55 deg.

For experiments a standard sensor chip CM5 from Biacore AB with a thickness of the gold film of 47 nm was used. To provide an optical contact between the film substrate (glass slide) and the glass prism a matching fluid was used. Due to the conversion of the energy of the incident light into SPs the reflected beam exhibited a dip at the SPR angle (Fig. 2) in the dependence of the reflected intensity versus incidence angle (SPR curve). A slit SL2 (Fig. 1) in front of the photodiode allowed selecting light propagating at different angles after interaction with the gold film and thus corresponding to certain portions of the SPR curve. Alternatively, the light reflected in the interval of angles around the SPR minimum was detected by a CCD camera. In this way a significant portion of the whole SPR curve could be measured. The CCD camera was also used for adjustments and for obtaining a well-pronounced SPR resonance.

B. Probing with SPR

The position of the SPR dip is sensitive to dielectric properties of the metal film and the adjacent media within the penetration depth of the SP electromagnetic field, which is typically less than a wavelength. The laser-induced variations of the dielectric properties of the metal result in a transformation of the SPR curve that can be quantified and gives a measure of the signal. The SPR probe response time is determined by the lifetime of SPs (about 60 fs for 800 nm), and the sensitivity is increased many fold due to resonance. The high sensitivity of this method is illustrated by the following calculation (see Fig. 2). In this and in the following calculations the dielectric constant of gold at $\lambda \approx 800$ nm was assumed to be $\varepsilon = -26 + 1.86i$. An increase of the dielectric constant of the gold film by 7% (i.e., both the real, ε_r, and imaginary, ε_i, parts of the metal dielectric constant are multiplied by 1.07) leads to the modification of the SPR curve as shown in Fig. 2. If two positions of the photodiode, PD1 and PD2, are considered, corresponding to collection of light within small angular intervals at the steep portions of the SPR curve, shown by vertical lines in Fig. 2, then the normalized change of the reflected intensity will be (−0.25) at PD1, and it will be (+0.31) at PD2. For comparison, for the same

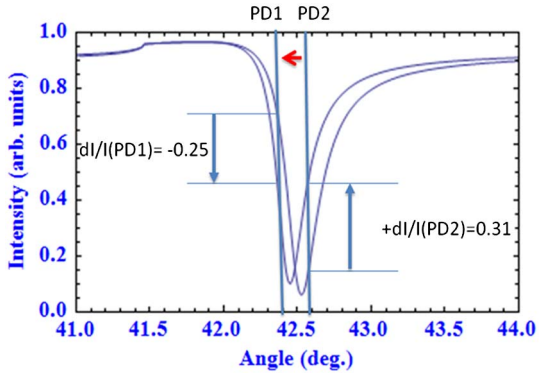

Fig. 2. Example showing changes in the normalized reflected intensity at the SPR with cw radiation at 800 nm induced by a 7% increase of the dielectric constant of the gold film. The red arrow indicates the direction of the shift of the SPR curve. The blue arrows indicate the sign and the magnitude of the relative changes of the intensity on two photodiodes, positioned on the steep slopes of the SPR curve, as indicated by the vertical blue lines. The step in the SPR curves occurring at ~41.5 deg is due to the total internal reflection.

7% variation of the dielectric constant and the same incidence angle of 42.55 deg a relative change of the intensity of the pulse reflected from the gold film interface with air, where no SPR is present, is only about 0.0022 according to Fresnel formulas. Consequently, the sensitivity of the SPR detection is about 250 times higher if two photodiodes are used in a differential scheme, and about 110 times higher for one photodiode at position PD1.

Another remarkable property of the SPR probe is its ability to predominantly measure contributions of the variations of real $\varepsilon_r = \mathrm{Re}(\varepsilon)$ or imaginary $\varepsilon_i = \mathrm{Im}(\varepsilon)$ parts of the metal dielectric constant. For illustration, a comparison of SPR curves calculated for $1.07\varepsilon_r$ and ε_r (no change in ε_i) is shown in Fig. 3(a), and the SPR curves for $1.07\varepsilon_i$ and ε_i (no change of ε_r) are depicted in Fig. 3(b). In the first case primarily an angular displacement of the SPR curves takes place, while in the second case the value of the SPR curve minimum primarily changes. In the assumption of small relative changes, this means that a photodiode positioned in the vicinity of the bottom of the SPR curve will mainly respond to the changes of ε_i, while for its positioning at the steep slope of the SPR curve the response will be mainly to changes of ε_r.

When a short probe pulse containing an interval of optical frequencies is used as a probe, the SPR response is somewhat different compared to a monochromatic laser probe. If the width of the SPR resonance is narrower than the bandwidth of the pulse, then different spectral components will have different reflectivities, and consequently the spectral and temporal distributions of the reflected pulse will be noticeably changed compared to the initial pulse, incident at the SPR angle. The spectral density of a reflected probe pulse, which at incidence is assumed to be a 50 fs Gaussian pulse, is shown in Fig. 4(a). The spectrally integrated angular dependence of the

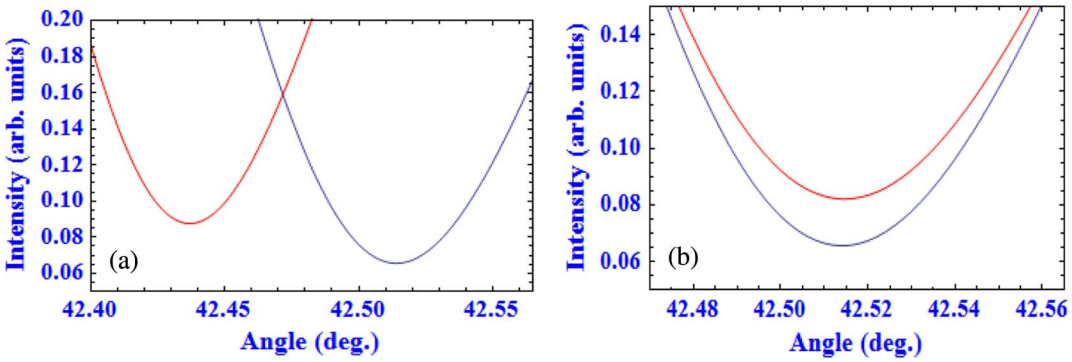

Fig. 3. Shift of the SPR curve in response to a 7% change of (a) ε_r, (b) ε_i. Blue curves show the initial position; red curves show changed position. Note a predominantly angular shift for a change of ε_r and a predominantly intensity (vertical) shift for a change of ε_i.

reflection coefficient is presented in Fig. 4(b). The angular minimum in the reflected pulse is shifted for different wavelengths. Since according to Parseval's equality the integral of the temporal distribution of the intensity is equal to the integral of the spectral density, the shift of the spectral distribution with the wavelength results in modification of the angular dependence of the total reflectivity, leading to a shallower minimum as illustrated in Fig. 4(b). For even shorter pulses the spectrum is broader and the decrease of the SPR dip becomes more pronounced.

In the general case, when changes of both the real and imaginary parts of the dielectric constant take place and cannot be assumed small, they can be found by fitting the measured SPR curve with a well-established Kretschmann model for the SPR in a layered system with a metal film [14]. We calculated in quadratic approximation for $\Delta\varepsilon_{r,i} \le 1$ the following dependences for variations of the position of the SPR minimum, $\Delta\theta_{\min}$ (in degrees), and the change of the reflectivity value at the minimum, $\Delta R_{\min}$, as functions of the variations of the real part $\Delta\varepsilon_r$ and the imaginary part $\Delta\varepsilon_i$ of the dielectric function of the metal. For a monochromatic 800 nm radiation we obtained

$$\begin{aligned}
\Delta\theta_{\min}(\Delta\varepsilon_r) &= 0.046\Delta\varepsilon_r + 1.1\times10^{-3}(\Delta\varepsilon_r)^2,\\
\Delta R_{\min}(\Delta\varepsilon_r) &= -0.0099\Delta\varepsilon_r + 1.1\times10^{-6}(\Delta\varepsilon_r)^2,\\
\Delta\theta_{\min}(\Delta\varepsilon_i) &= 0.0036\Delta\varepsilon_i + 0.0021(\Delta\varepsilon_i)^2,\\
\Delta R_{\min}(\Delta\varepsilon_i) &= 0.13\Delta\varepsilon_i - 0.0085(\Delta\varepsilon_i)^2,
\end{aligned} \tag{1}$$

and for a 50 fs pulse centered at 800 nm these dependences change somewhat:

$$\begin{aligned}
\Delta\theta_{\min}(\Delta\varepsilon_r) &= 0.050\Delta\varepsilon_r - 1.1\times10^{-3}(\Delta\varepsilon_r)^2,\\
\Delta R_{\min}(\Delta\varepsilon_r) &= -0.013\Delta\varepsilon_r + 0.00032(\Delta\varepsilon_r)^2,\\
\Delta\theta_{\min}(\Delta\varepsilon_i) &= 0.0020\Delta\varepsilon_i + 0.0040(\Delta\varepsilon_i)^2,\\
\Delta R_{\min}(\Delta\varepsilon_i) &= 0.085\Delta\varepsilon_i - 0.002(\Delta\varepsilon_i)^2.
\end{aligned} \tag{2}$$

Equations (1) and (2) show that indeed the variations $\Delta\varepsilon_r$ contribute predominantly to $\Delta\theta_{\min}$, and the variations $\Delta\varepsilon_i$ contribute predominantly to $\Delta R_{\min}$. A comparison of Eqs. (2) with Eqs. (1) shows that due to the finite bandwidth of the pulse the response in the angular shift of the SPR changes only slightly by ~9%, while the value at the SPR minimum changes significantly by ~35%.

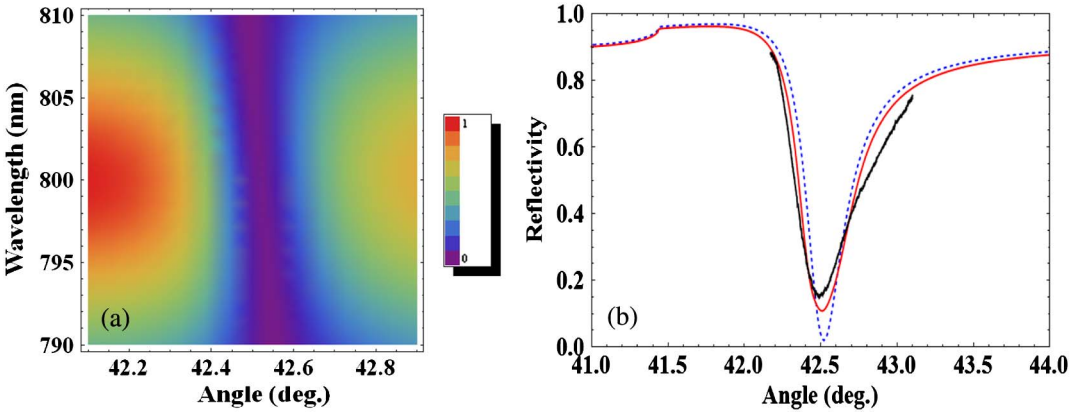

Fig. 4. Characteristics of the reflected probe pulse: (a) spectral density distribution: the angular position of the SPR is slightly shifted for different wavelengths; (b) angular dependence of the total reflectivity (solid red line). For comparison the reflectivity of a monochromatic 800 nm radiation is shown (dashed blue line); the experimental SPR curve is shown as a black solid line.

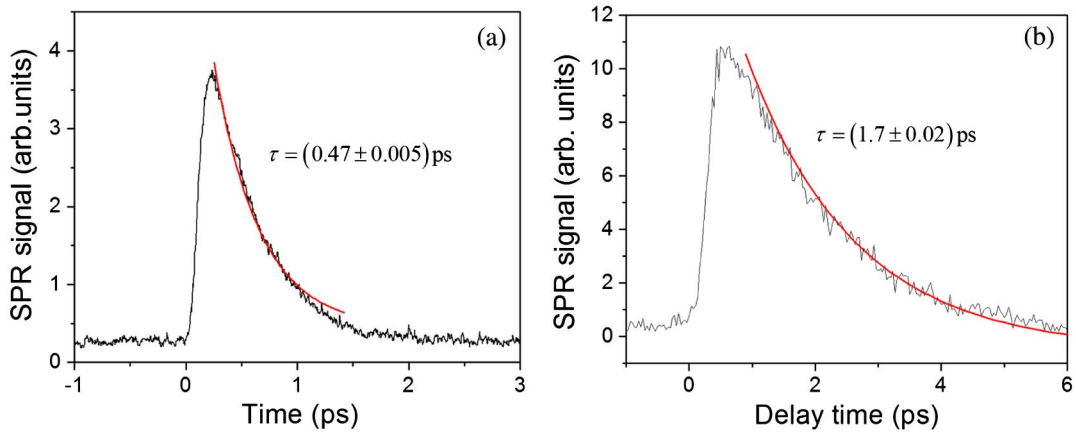

Fig. 5. Recorded relaxation signal after excitation by radiation of ~800 nm pump pulse with laser fluence (a) $F = 11$ mJ/cm^2 and (b) $F = 32$ mJ/cm^2. The SPR probe mainly registered changes in ε_r. The red solid lines show fits with an exponential decay, and the decay times are also shown.

3. Results

A. Experimental Results

The SPR signals for excitation pulses centered at 800 nm wavelength are shown in Fig. 5. In the measurement the slit was positioned to select an angular interval on the steep slope of the SPR curve, and the measured response corresponded predominantly to changes in ε_r. The initial peak is associated with the response to electronic excitations [4], followed by a long tail of the relaxation process. The rise time of the response was found to be about 60 fs [from the relative level of 0.25–0.75 on the rising slope of the peak, see Fig. 5(a)] and close to the response time expected from the SP lifetime and the pulse duration. The relaxation times of $\tau = (0.47 \pm 0.005)$ ps at the laser fluence $F = 11$ mJ/cm^2 and of $\tau = (1.7 \pm 0.02)$ ps at $F = 32$ mJ/cm^2 were found by fitting the declining slopes of the signals with exponential decay. The picosecond values of the relaxation time are typical for the electron-lattice thermalization process [1–5], and the observed increase of the relaxation time with the laser fluence is in agreement with previous observations [9,10].

When the photodiode detected light corresponding to the vicinity of the SPR dip (see Fig. 6), the signal also exhibited a sharp peak, originating from the initial electronic excitations and the following decay due to the electron–phonon relaxation. The signal did not return to the initial level, indicating that the complete relaxation to the initial state was not reached within the observation time interval. It was observed that the shift of the signal level was increasing with the pump laser fluence. The observed oscillations in the tailing part of the signal result from the excitation of acoustic oscillations in the film [9,11]; the period of these oscillations of about 28 ps compares favorably with the calculated round-trip time of 29 ps of a longitudinal acoustic wave in the gold film in the normal to the surface direction.

With a similar arrangement the combined action of 800 and 400 nm pulses was also measured (Fig. 7). In this case no filter was inserted in the pump beam after the SHG crystal. Although the calculated density of the energy deposition for the second pulse is smaller than for the first pulse, the relaxation time after its action is longer, which apparently is related to a preheating effect produced by the first pulse. We note that although a 400 nm pulse is much less energetic than the 800 nm pulse, due to a much higher absorbance at 400 than at 800 nm the SPR responses for both pulses are comparable.

B. Two-Temperature Model

The dynamics of the electron-lattice relaxation were simulated with the two-temperature model [15,16] by two coupled equations for the temperatures of the electrons and the lattice,

$$C_e \frac{dT_e}{dt} = -g(T_e - T_l) - K_e B(T_e - T_{\text{env}}) + Q(t), \quad (3)$$

$$C_l \frac{dT_l}{dt} = g(T_e - T_l) - (T_l - T_{\text{env}})/\tau_l, \quad (4)$$

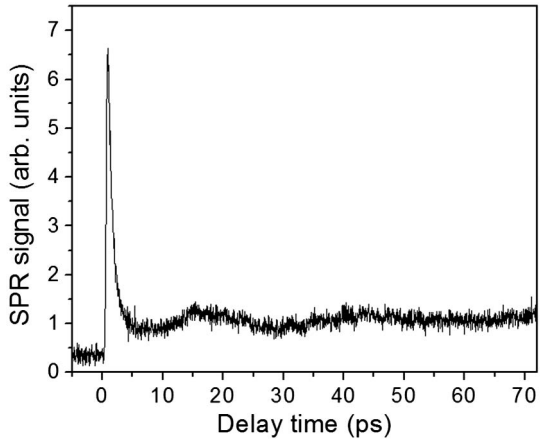

Fig. 6. Recorded relaxation signal after excitation by a 400 nm pulse with a laser fluence $F = 2.1$ mJ/cm^2.

where T_e and T_l are the electronic and lattice temperatures, respectively; C_e and C_l are the corresponding specific heat capacities of the electronic subsystem and the lattice; g is the electron–phonon coupling parameter; and $Q(t)$ is the absorbed laser energy density deposited in the electronic subsystem. We used the following approximation for the electronic thermal conductivity, $K_e = K_{e0}(T_e/T_l)$ [16,17], and took into account the dependences of C_e and g on the electron temperature, which become significant at high excitation levels [18]. These dependences were approximated in the range of electronic temperatures 273 K $< T_e <$ 10^4 K by the following expressions:

$$g(T_e) = g_0[1 + f_2(T)],$$
$$f_2(T) = 14[(T_e/T_2)^{2.8}/[1 + (T_e/T_2)^{2.8}], \quad (5)$$

$$C_e(T_e) = A_e T_e[1 + f_1(T_e)],$$
$$f_1(T_e) = 2.5(T_e/T_1)^4/[1 + (T_e/T_1)^4]\exp(-T_e/T_3), \quad (6)$$

where $g_0 = 2.0 \times 10^{16}$ W/m^3 K, $T_1 = 5.5 \times 10^3$ K, $T_2 = 10^4$ K, and $T_3 = 4 \times 10^4$ K. The following parameters were used for simulations [16]: $Q(t) = Q_0 \exp[-(t - t_0)^2/\tau_1^2]$, where $Q_0 = AF/(\sqrt{\pi}\tau_1 d)$ with the absorptivity $A = 0.04$ for 800 nm and $A = 0.74$ for 400 nm; the laser fluence F is indicated for each calculation separately; $\tau_1 = (\tau/2\sqrt{\ln(2)})$, where the pulse duration is $\tau = 50$ fs; $d = 47$ nm was accepted to be equal to the film thickness due to fast heat propagation with ballistic electrons [16], since their typical propagation distance of about 100 nm is larger than the film thickness and the penetration depth l_p of the laser radiation ($l_p = 12$ nm for 800 nm and $l_p =$ 16 nm for 400 nm); $t_0 = 0.5$ ps for the 800 nm pulse and $t_0 = 1.8$ ps for the second pulse at 400 nm (see below); parameter $B \lesssim 2.4 \times 10^{-6}$ nm^{-2}, which depends on the electron temperature and its gradient, was found by fitting; $\tau_l = 45$ ns, $K_{e0} = 318 \times 10^6$ W/mK, $A_e = 68$ J/m^3 K^2, $T_{\text{env}} = 300$ K.

4. Discussion

The excitation and relaxation of a gold film is observed with femtosecond pulses in a pump–probe scheme using a pulsed SPR probe. The measured fast rise times of the signal show that indeed the SPR probe provided high temporal resolution determined by the SP lifetime and the laser pulse duration.

The presented calculations show that the probe signal responds to changes of different physical quantities, depending on the interval of the reflection angles of the probe beam that is used for the detection. If the portion of the SPR reflection curve corresponding to the steep slope is selected, then the signal reflects predominantly the variations of the real part of the metal dielectric constant. Indeed, the shapes of the observed signals in Figs. 5(a) and 5(b) closely resemble the temporal dependences obtained for the real part of the metal dielectric constant in pump–probe experiments [4]. The variations $\Delta\varepsilon_r$ are closely related to the changes of the thermal energy of the electron gas; in particular for relatively small temperature variations, it was shown that the change of the real part of the metal dielectric constant $\Delta\varepsilon_r$ is proportional to the total thermal energy of the electron gas [2,10].

Above we have shown that when the reflected probe light near the SPR minimum is selected, mainly variations of the imaginary part of the metal dielectric constant are registered. However, a comparison of the shapes of the measured signals in Figs. 6 and 7 with the temporal behavior of ε_i in pump–probe experiments [4] suggests that measured signals contain contributions of both $\Delta\varepsilon_r$ and $\Delta\varepsilon_i$. Both contributions of $\Delta\varepsilon_r$ and $\Delta\varepsilon_i$ are reflected in the signal instead of just the one from $\Delta\varepsilon_i$ because, first, the selected interval is not quite symmetric relative to the SPR minimum; second, the SPR curve is also not symmetrical; and, third, as Eqs. (2) show, the changes of ε_r also contribute to variations of the ΔR_{min}, although less than those of ε_i. At 400 nm interband transitions are induced, since the photon energy of 3.1 eV exceeds the energy for a transition from the d-band to the vicinity of the Fermi level (~2.4 eV in Au). The variation of $\Delta\varepsilon_i$ owing to the interband transitions can be found as the product of the square of the momentum matrix element between the d-band and the Fermi level and the joint density of states for d-band-to-conduction-band transitions [19,20], and through the Kramers–Kronig relation the respective variation of ε_r can also be calculated. The interband excitations have a short lifetime, in the range of 1–100 fs [4,21], and manifest themselves as a sharp spike in the ε_i of this short duration [4,22]. In the signals in Figs. 5 and 6 the contribution of the interband transitions can be masked by the steep rising front of the $\Delta\varepsilon_r$ contribution. It should be possible to determine $\Delta\varepsilon_r$ and $\Delta\varepsilon_i$ separately by registering SPR curves for different probe delays, determining $\Delta\theta_{\text{min}}$ and ΔR_{min}, and solving Eqs. (2) for $\Delta\varepsilon_r$ and $\Delta\varepsilon_i$; however, this is beyond the scope of this paper.

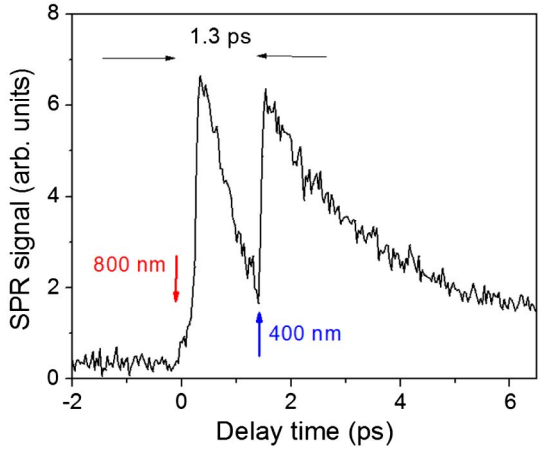

Fig. 7. Recorded relaxation signal after excitation by a pulse at 800 nm, $F = 60$ mJ/cm^2, followed with a 1.3 ps delay by a pulse at 400 nm, $F = 1.4$ mJ/cm^2.

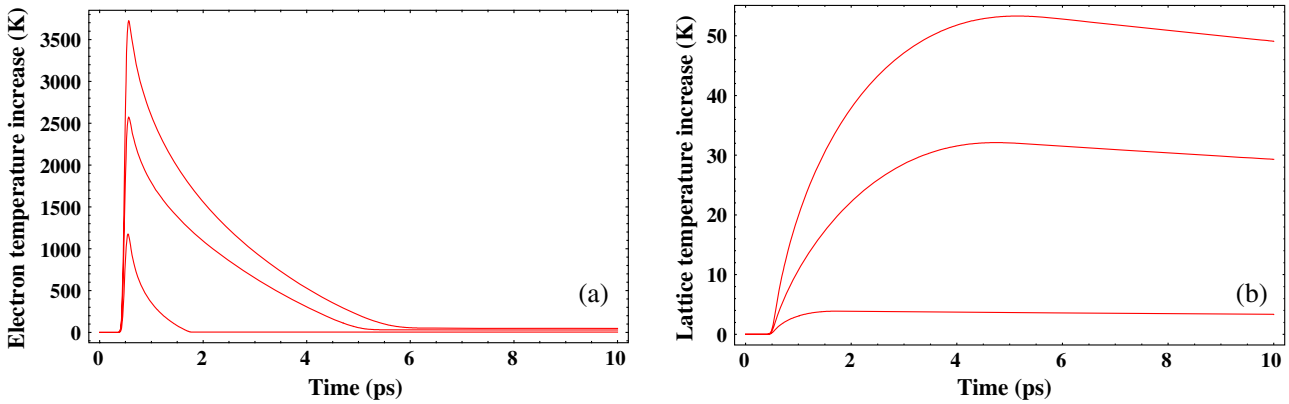

Fig. 8. Calculated temporal dependences of (a) electron temperature and (b) lattice temperature for three laser fluences of the incident beam at 800 nm (from bottom to top): $F = 10, 30, 80$ mJ/cm^2.

The shift of the signal level in the tailing portion of the pulse (see Figs. 5 and 6), which is observed on a long time scale (we observed it up to hundreds of picoseconds), results from the heating of the lattice due to intraband transitions and the respective increase of the electron scattering rate [10,20].

The increase of the relaxation time with the level of the excitation is documented in previous studies [2,16] and can be related to increasing thermal capacity of the electron gas with increasing electron temperature. Here we take into account dependences of the electron–phonon coupling and thermal capacity of the electronic subsystem on electron temperature and can reproduce electron relaxation times quite well: for $F = 10$ and 30 mJ/cm^2 the experimentally determined relaxation times (at $1/e$ level) found by exponential fitting are 0.47 and 1.7 ps, respectively, while the TTM calculations gave values 0.45 and 1.8 ps, respectively.

In [16], the linear portion of the relaxation dependence was observed for thin films and related to the heat conduction by ballistic electrons with a mean free path about 100 nm. The measured relaxation dependences of Figs. 4(a) and 4(b) are well described by exponential fits, and simulations (see Fig. 8) show that taking into account the dependences of the electron–phonon coupling constant and the electronic subsystem heat capacity on the electronic temperature as well as the heat conduction flux is important. Additional comparison with the TTM model was performed for dependences of Fig. 7, observed for double-pulse excitation. The experimental first (0.68 ± 0.01 ps) and second (2.6 ± 0.03 ps) relaxation times are close to the relaxation times of 0.88 and 2.2 ps found with the same model of Eqs. (3)–(6) applied to this case (Fig. 9). In Fig. 7 the second (400 nm) pulse is incident when the equilibration of the electronic subsystem and the lattice is not yet reached and the electronic temperature is still significantly higher than the equilibrium value. The second pulse has much lower energy, but the absorbance of gold at 400 nm of 0.74 is much higher than the absorbance of 0.04 for 800 nm. Consequently, the second pulse produces a peak in the probe beam signal comparable to the one of the first pulse. The relaxation time after the second peak is longer, which agrees with the increase of the electronic temperature obtained also in the simulation [Fig. 9(a)] and also with the growth of the thermal capacity of the electrons according to Eq. (6).

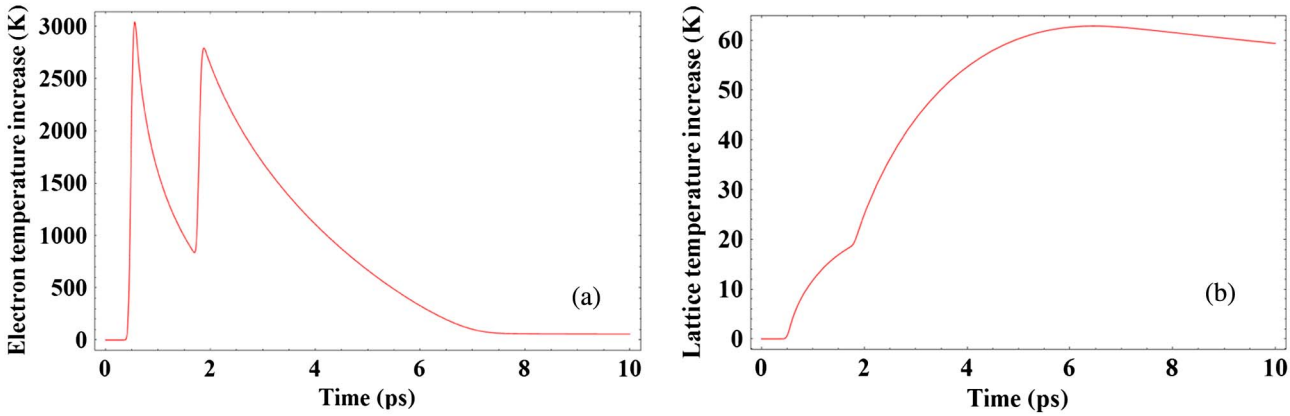

Fig. 9. Calculated temporal dependences of (a) electron temperature and (b) lattice temperature for a dual pulse excitation with incident fluences $F = 60$ mJ/cm^2 (800 nm) and $F = 1.0$ mJ/cm^2 (400 nm).

5. Conclusion

An SP probe allows monitoring of laser-induced changes in metal films with high temporal resolution and sensitivity. By selecting certain angular intervals near the angle of the SPR it is possible to predominantly detect the changes of the real or imaginary part of the dielectric constant of the metal; that is, detection at the steep slope of the SPR curve responds mainly to changes of the real part, while detection near the dip of the SPR curve enhances the response to changes of the imaginary part of the metal dielectric constant. Due to the probe laser pulse bandwidth, a noticeable change in the SPR curve takes place, which is especially pronounced in the amount of light reflected at the resonance angle (about 35% change). In experiments with the SP probe, a temporal resolution of about 60 fs was determined by the duration of the laser pulse and the lifetime of the SPs. The relaxation times were measured in the range 0.5–2.6 ps, increasing with the level of the excitation, which was also confirmed by the calculations with the TTM. A combined excitation by two pulses at 800 and 400 nm with subsequent relaxation dynamics was experimentally observed and simulated with the TTM, taking into account temperature dependences of the electronic heat capacity and the electron–phonon coupling.

This work was supported in part by the Robert A. Welch Foundation (grant no. A1546) and the National Science Foundation (grant no. 0722800).

References

1. R. W. Schoenlein, W. Z. Lin, J. G. Fujimoto, and G. L. Eesley, "Femtosecond studies of nonequilibrium electronic processes in metals," Phys. Rev. Lett. **58**, 1680–1683 (1987).
2. C.-K. Sun, F. Vallée, L. H. Acioli, E. P. Ippen, and J. G. Fujimoto, "Femtosecond-tunable measurement of electron thermalization in gold," Phys. Rev. B **50**, 15337–15348 (1994).
3. H. Inouye and K. Tanaka, "Ultrafast dynamics of nonequilibrium electrons in a gold nanoparticle system," Phys. Rev. B **57**, 11334–11340 (1998).
4. N. Del Fatti, C. Voisin, M. Achermann, S. Tzortzakis, D. Christofilos, and F. Vallée, "Nonequilibrium electron dynamics in noble metals," Phys. Rev. B **61**, 16956–16966 (2000).
5. B. Rethfeld, A. Kaiser, M. Vicanek, and G. Simon, "Ultrafast dynamics of nonequilibrium electrons in metals under femtosecond laser irradiation," Phys. Rev. B **65**, 214303 (2002).
6. W. S. Fann, R. Storz, H. W. K. Tom, and J. Bokor, "Electron thermalization in gold," Phys. Rev. B **46**, 13592–13595 (1992).
7. X. Y. Wang, D. M. Riffe, Y.-S. Lee, and M. C. Downer, "Time-resolved electron temperature measurement in a highly-excited gold target using femtosecond thermionic emission," Phys. Rev. B **50**, 8016–8019 (1994).
8. M. Kiel, H. Mohwald, and M. Bargheer, "Broadband measurements of the transient optical complex dielectric function of a nanoparticle/polymer composite upon ultrafast excitation," Phys. Rev. B **84**, 165121 (2011).
9. R. H. M. Groeneveld, R. Sprik, and A. Lagendijk, "Effect of nonthermal electron distribution on the electron–phonon energy relaxation process in noble metals," Phys. Rev. B **45**, 5079–5082 (1992).
10. R. H. M. Groeneveld, R. Sprik, and A. Lagendijk, "Femtosecond spectroscopy of electron–electron and electron–phonon energy relaxation in Ag and Au," Phys. Rev. B **51**, 11433–11445 (1995).
11. J. Wang and C. Guo, "Effect of electron heating on femtosecond laser-induced coherent acoustic phonons in noble metals," Phys. Rev. B **75**, 184304 (2007).
12. K. F. MacDonald, Z. L. Sámson, M. I. Stockman, and N. I. Zheludev, "Ultrafast active plasmonics," Nat. Photonics **3**, 55–58 (2008).
13. P. Vasa, C. Ropers, R. Pomraenke, and C. Lienau, "Ultra-fast nano-optics," Laser Photon. Rev. **3**, 483–507 (2009).
14. E. Kretschmann, "Die Bestimmung optischer Konstanten von Metallen durch Anregung von oberflichenplasmaschwingungen," Z. Phys. **241**, 313–324 (1971).
15. S. I. Anisimov, B. L. Kapeliovich, and T. L. Perelman, "Electron emission from metal surfaces exposed to ultrashort laser pulses," Sov. Phys. J. Exper. Theor. Phys. **39**, 375–377 (1974).
16. J. Hohlfeld, S.-S. Wellershoff, J. Güdde, U. Conrad, V. Jähnke, and E. Matthias, "Electron and lattice dynamics following optical excitation of metals," Chem. Phys. **251**, 237–258 (2000).
17. M. Bonn, D. N. Denzler, S. Funk, and M. Wolf, "Ultrafast electron dynamics at metal surfaces: competition between electron–phonon coupling and hot-electron transport," Phys. Rev. B **61**, 1101–1105 (2000).
18. Z. Lin and L. V. Zhigilei, "Thermal excitation of d band electrons in Au: implications for laser-induced phase transformations," Proc. SPIE **6261**, 62610U (2006).
19. R. Rosei, "Temperature modulation of the optical transitions involving the Fermi surface in Ag: theory," Phys. Rev. B **10**, 474–483 (1974).
20. R. D. Averitt, S. L. Westcott, and N. J. Halas, "Ultrafast optical properties of gold nanoshells," J. Opt. Soc. Am. B **16**, 1814–1823 (1999).
21. E. V. Chulkov, A. G. Borisov, J. P. Gauyacq, D. Sánchez-Portal, V. M. Silkin, V. P. Zhukov, and P. M. Echenique, "Electronic excitations in metals and at metal surfaces," Chem. Rev. **106**, 4160–4206 (2006).
22. A. Devizis and V. Gulbinas, "Ultrafast dynamics of the real and imaginary permittivity parts of a photoexcited silver layer revealed by surface plasmon resonance," Appl. Opt. **47**, 1632–1637 (2008).